

Improvements in Wear and Corrosion Resistance of RB400 Anchor Rod Steel by Electroless Ni-P Plating

Naiming Lin^{1,*}, Hongyan Zhang¹, Jiaojuan Zou¹, Pengju Han², Yong Ma¹, Bin Tang¹

¹ Research Institute of Surface Engineering, Taiyuan University of Technology, Taiyuan, 030024, P. R. China

² Department of Civil Engineering, Taiyuan University of Technology, Taiyuan, 030024, P. R. China

*E-mail: lnmlz33@126.com

Received: 11 October 2014 / Accepted: 5 November 2014 / Published: 17 November 2014

Engineering components with high wear and corrosion resistant surfaces are essentially required to meet the ever-increasing demands for rapid developments of engineering applications upon the subjections to complex and/or harsh conditions. For example, there are needs for supporting anchor rods in to resist both corrosion and wear attacks during operation. In the present work, electroless plating was employed to prepare Ni-P coating on RB400 steel for improving surface performance and increasing usage of anchor rod in bracing project. Surface and cross-section morphologies of the obtained coating were measured by scanning electron microscope (SEM) and optical microscope (OM). Phase constitution and sectional element distribution were analyzed by X-ray diffraction (XRD) and glow discharge optical emission spectrometry (GDOES). A ball-on-disc type tribometer and electrochemical workstation were applied to make comparative evaluations on wear and corrosion resistance of anchor rod steel and Ni-P coating, respectively. The results showed that uniform and compact Ni-P coating was formed on RB400 steel anchor rod substrate. The surface hardness of substrate had tripled after electroless plating treatment. The obtained Ni-P coating indicated good antifriction effect and possessed excellent wear resistance, which was validated by friction coefficient, mass loss and worn-out appearance. The Ni-P coating exhibited higher corrosion potential and lower corrosion current density in comparison with bared anchor rod. The surface performance of anchor rod steel was significantly improved by Ni-P coating.

Keywords: Wear; corrosion; RB400 steel; anchor rod; electroless plating; Ni-P coating

1. INTRODUCTION

The underground support engineering is a concealed work [1]. As vital support material, anchor rods (as shown in Figure 1) [2–5], generally used in various fields as laneway, mine, tunneling and

rock slope engineering, play an important role in the construction and safety aspects. However, the anchor rods are prone to deteriorate under complex and adverse geological conditions [1, 6–8]. Wear and corrosion are the main failure modes for anchor rods working under such circumstances. As a result, the method to improve the surface corrosion and wear resistance of anchor rods steel has attracted the attention of many researchers.

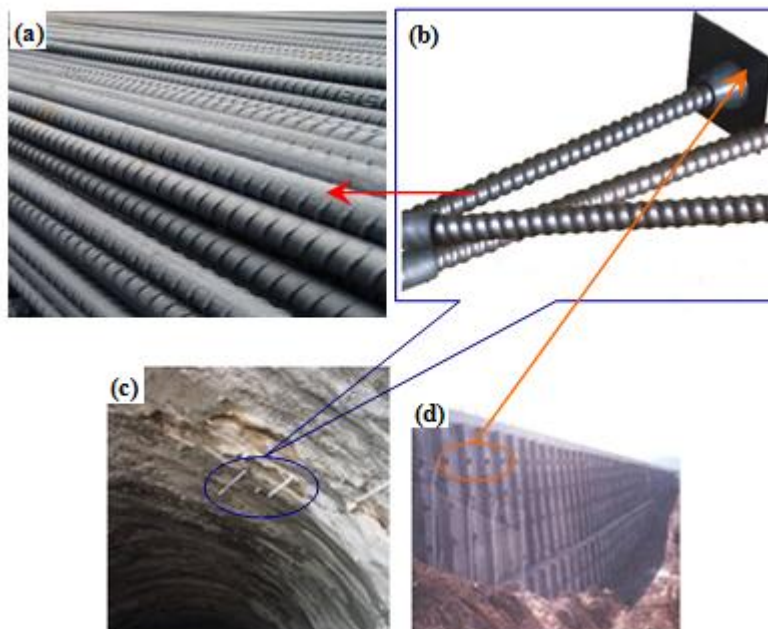


Figure 1. Anchor rods applied in engineering as vital support materials

For protection of anchor rods steel against corrosion, various types of surface modification have been proposed. Maldonado and Pech-Canul have reported the performance of hot-dip zinc-coated steel rebars embedded in concrete which was exposed to tropical humid marine environments [9]. They found that the zinc-coated rebars remained passive for a period of two years in the case of concretes with a water/cement ratio which was less than 0.6. However, the zinc-coated rebars with a water/cement of 0.7 appeared to corrode in the fourteenth month. Bellezze et al. studied the corrosion performance of three different galvanized steel rebars (Zn-Pb; Zn-Ni-Bi; and Zn-Ni-Sn-Bi baths) embedded in concrete [10]. The bars galvanized in Zn-Ni-Sn-Bi bath showed good corrosion resistance in concrete with low alkalinity and high chloride content while the corrosion performance in high alkaline concrete matrix is unsatisfactory. On the contrary the bars galvanized in Zn-Pb and Zn-Ni-Bi baths performed better in concrete with high alkalinity. Researchers also characterized the coating on rebar surface obtained from Zn-4.9Al-0.1 misch metal bath [11]. The epoxy-coated steel with good corrosion performances has also been reported [12].

The electroless plating Ni-P alloy technique is a well-known commercial process and has numerous applications in many fields due to excellent properties such as high corrosion resistance, high wear resistance, high hardness, good lubricity, acceptable ductility, and outstanding compatibility.

The electroless plating technique can be applied on different substrates as steel, aluminum alloy, magnesium alloy, copper, ceramics, carbon nanotube (CNT) and hydrophobic polymer etc. [13–18], various coatings have been induced with different needs as well [19]. Furthermore, the electroless plating technology has no special requirements for substrate geometries [20, 21]. While considering the simple and feasible operation of electroless plating, it shows good advantages in the large-scale production of components. The kinetics information about deposition process of electroless Ni-P coating was studied through its electrochemical behavior by Xie et al. they also discussed the influence of experiment parameter [22]. Mohammad Islam carried out the electrochemical impedance spectroscopy (EIS) and indentation tests of pure and composite electroless Ni-P coatings and investigated the addition effect on corrosion resistance and hardness of Ni-P-Al₂O₃, Ni-P-SiC and Ni-P-CNT composite coatings [23]. M. Yan et al. studied the microhardness and wear resistance of electroless Ni-P coating [24]. It revealed a high hardness of 910 HV_{0.1} on the Ni-P coating with 7.97 at. % phosphorus, accordingly high wear resistance was achieved. Especially, the deformation behavior of amorphous Ni-P coating was investigated using the Vickers indentation and evaluated fracture toughness. Besides, a preferential annealing temperature was proposed to balance the hardness, brittleness and corrosion resistance of the coating [25].

In addition to academic research about the technology and performance of various electroless plating coatings, the actual applications of electroless plating have been actualized in many different ways. Y.H. Cheng actualized electroless Ni-P plating technology on heat transfer device and studied the effect of microstructure on the performance of the Ni-P coatings [26]. The amorphous Ni-P coating exhibits high corrosion resistance, which attributed to its extreme structure homogeneity without preferential corrosion paths like grain boundaries or other structural defects. The higher corrosion resistance could make it not easy to form “transitional interface” between fouling and matrix. C.K. Lee evaluated the mechanical, electrochemical and wear-corrosion properties of electroless nickel-phosphorus coatings on carbon-fiber-reinforced plastic (CFRP) composites commonly used in aeronautical and astronautical applications due to their superior properties such as high specific strength and modulus [27]. Moreover, the corrosion and wear-corrosion resistance of electroless Ni-P coating on glass fiber-reinforced plastic (GFRP) composites, frequently used in wind turbine blades, were also evaluated [28]. The study on corrosion performance of electroless Ni-P alloy coatings applied on steel rebars embedded in concrete, conducted by Singh and Ghosh, has indicated a high degree of protection [29]. Excellent corrosion performances of polyaniline/nylon composites coating on steel was found by Ansari and Alikhani [30]. The polyaniline/nylon coating can provide an anodic protection for steel against corrosive environments with corrosion rate which is 10~15 times lower than the bare steel. Lin et al. had reported excellent performance of coating against chloride-induced corrosion under the action of silane coupling agent and rare earths [31]. M. Manna et al. investigated the effect of plating time on electroless Ni alloy coating of rebar, as well as the applicability in concrete structure [32]. Matteo Gastaldi et al. compared the effect of temperature (in the range of 20~60 °C) on the resistance to chloride-induced corrosion of low-nickel duplex stainless steel rebars and traditional austenitic stainless steel rebars, respectively [33]. All of the above findings confirmed that electroless plating Ni-P coating could enhance the wear and corrosion resistance of the treated base materials with promising contour feature.

The present study aims (i) to form Ni-P coating on RB400 steel anchor rod via electroless plating process to improve the surface performance and increase the usage lifetime during operation; (ii) to characterize the surface morphology and element distribution, cross-sectional microstructure and phase constitutions of the Ni-P coating; and (iii) to exam the wear and corrosion resistance of the Ni-P coating.

2. EXPERIMENTAL PROCEDURES

2.1. Deposition of Ni-P coating

As a common type of anchor rod, reinforced bar RB400 steel was chosen for the experiments. The chemical composition of RB400 (in wt. %) was 0.23% C, 1.42% Mn, 0.63% Si, 0.037% P, 0.033% S and the balance Fe. The samples were cut into a size of Φ 18 mm \times 3 mm as substrate by an electro-spark wire-electrode cutting machine. The surfaces were finely ground on SiC abrasive papers to 1000 grit size, followed by ultrasonic cleaning in acetone bath. All the samples were subjected to the following pre-treatment and plating procedure:

1. Cleaning in alkaline solution containing 70 g/L sodium hydroxide, 40 g/L sodium carbonate, 20 g/L sodium phosphate, and 10 g/L sodium silicate, at the temperature of 85 °C for 5 min.
2. Immersion in distilled water at room temperature (RT) for 2 min.
3. Cleaning in 20 vol. % HCl at RT for 1~2 min.
4. Rinsing by immersion in distilled water at RT for 2 min.
5. Cleaning in 5 vol. % H₂SO₄ at RT for 1 min.
6. Rinsing by distilled water at RT for 2 min.
4. Electroless plating, dipping into plating bath whose composition and correlative parameters are given in Table 1.
6. Rinsing by distilled water at RT for 2 min, and drying in the air.

Table 1. Electroless plating bath composition

Compound	Concentration (g/L)
NiSO ₄ · 7H ₂ O	40
NaH ₂ PO ₂	25
Sodium citrate	45
sodium acetate	40
pH	4.5–6.0
T/°C	85–88

2.2. Characterizations and testing

Scanning electron microscope (SEM) with energy dispersive X-ray spectrometer (EDS) was employed to investigate the surface morphologies and microstructures. The phase constitution of the

obtained coating was determined by X-ray diffraction (XRD, Philips X'Pert Pro) using Cu K α radiation (1.5410Å wavelength). Depth profile analysis of the plated samples was performed using glow discharge optical emission spectrometry (GDOES).

Tribological behaviors of RB400 substrate and the deposited Ni-P coating were conducted on the MFT-R4000 reciprocating friction and wear tester in dry sliding. High carbon chromium bearing steel balls with the diameter of 5 mm was chosen as the counterparts. All the tests were conducted at RT with a normal load of 5 N and 20 N for 30 min under a sliding velocity of 224 r/ min. The wear resistance of the samples was characterized through the comparison of friction coefficient, mass loss and the wear trace. The mass loss values of original and worn samples were estimated by an analytical balance with an accuracy of 0.01 mg. The topographical features of the worn surfaces were examined using SEM.

Corrosion studies were conducted using electrochemical measurement system (CS350 CorrTest). The corrosion cell was combined with a typical three-electrode configuration. The saturated calomel electrode (SCE) was used as reference electrode while bare and coated samples with a naked geometric area of 1 cm² and a platinum plate were chosen as working electrodes and counter electrode respectively. All the tests were carried out at room temperature, including the test of open circuit potential (OCP), potentiodynamic polarization (the curves were swept from 0.5 V to 1.5 V vs OCPs. with a scan rate of 0.5 mV/s) and electrochemical impedance spectroscopy (EIS)

3. RESULTS AND DISCUSSION

3.1. Microstructural characterizations

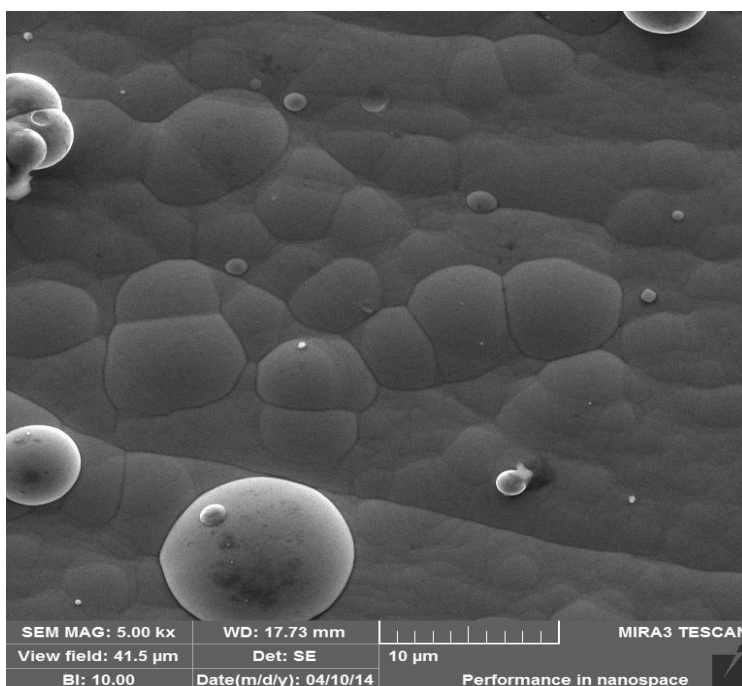


Figure 2. Surface morphology of as-plated Ni-P coating

The Ni-P coating exhibits a silver-grey surface by naked-eye glance. Figure 2 presents the surface morphology of Ni-P coating. It is clear that the obtained coating is uniform and compact. Its unique nodular microstructure resemble that of cauliflower-like [20], indicating a typical characteristic of Ni-P coating that formed by electroless plating process [34].

The phase composition of the Ni-P coating is analyzed by XRD pattern (Figure 3). Only a single and broad diffraction peak ($2\theta \approx 45^\circ$) can be found from the pattern. X-ray diffraction is formed through the crystal faces fitting the Bragg diffraction angel. The deposits are amorphous with little crystalline microstructure and show broad peaks. The broadening of the peaks is mainly attributable both to microstress and microcrystalline structure or amorphous structure of Ni-P films being supersaturated with respect to phosphorus [35, 36]. By comparison with the XRD diffraction profile cards, the coating was composed of amorphous and microcrystalline nickel. According to the characteristics of amorphous, the coating also has excellent thermal stability.

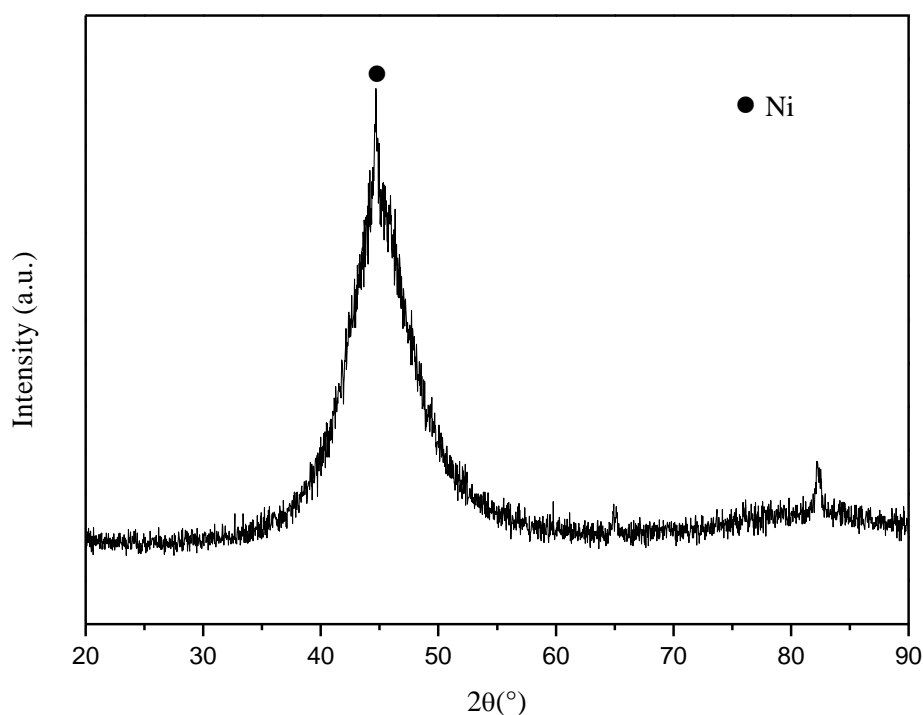


Figure 3. XRD pattern of as-plated Ni-P coating

Figure 4 shows cross-section morphology of the Ni-P coated sample. The uniform thickness of the coating can be estimated as 16 μm through the scaleplate. The characterization method of GDOES can not only analyze all the contained elements and their contents on the coating, but also check the distribution trend of elements with depths from the surface to substrate. The elemental distribution state of the Ni-P coating (Figure 5) indicates that only main elements Ni and P are contained in the coating. Meanwhile their compositions remain stable, which reveals that the coating was evenly distributed. In the depth ranges of 15~20 μm , the elements of coating decrease gradually, thus the thickness of coating can be judged. As can be seen, this result is consistent with the cross-section

scanning image. According to the content of P in the coating (6 wt. %), the protective Ni-P coating on the anchor rod through the electroless plating can be classified as medium-phosphorus coating. The protection performances of coating need to be explained by the specific test under certain conditions.

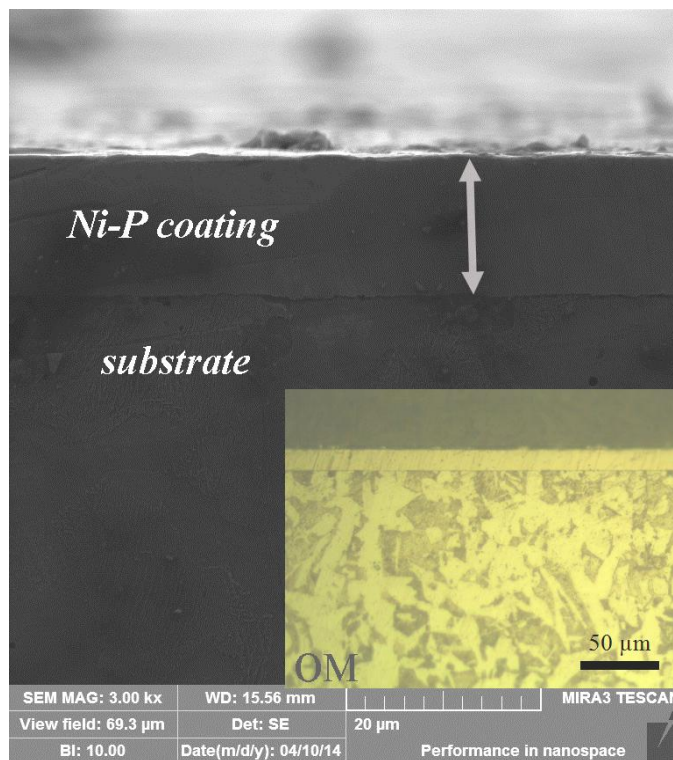


Figure 4. Cross section morphology of the Ni-P coating

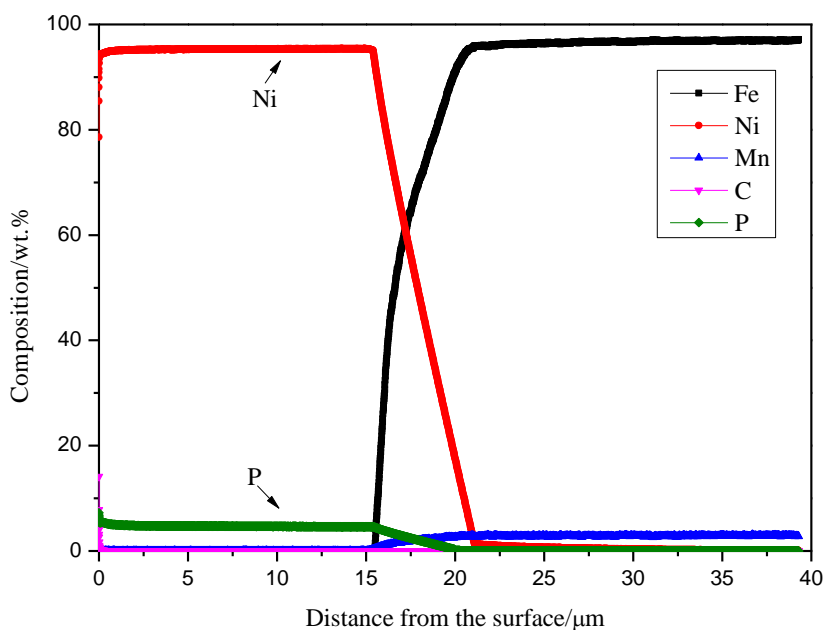


Figure 5. Glow discharge optical emission spectrometry (GDOES) profile of as-plated Ni-P coating

3.2. Hardness of Ni-P coating

Hardness is one of the most commonly used indexes for evaluation of mechanical properties of metal material. The hardness of electroless plating coating directly affects the applicability of the studied material. As the bolt surface is the main contact area during service process, we choose the surface micro hardness test. The final dates are gotten by averaging the microhardness of five different positions on surface of substrate and Ni-P coating. It is notable in Figure 6 that the Ni-P coating has higher surface hardness than that of RB400 steel substrate. Thus the microhardness of substrate material has tripled after electroless Ni-P plating treatment. The enhanced hardness is attributed to the featured composition and structures. Based on the existing research results, the general improvement of wear resistance can be inferred. Furthermore, the phosphorus content of this coating is proved to be appropriate to achieve high hardness of the Ni-P coating [37].

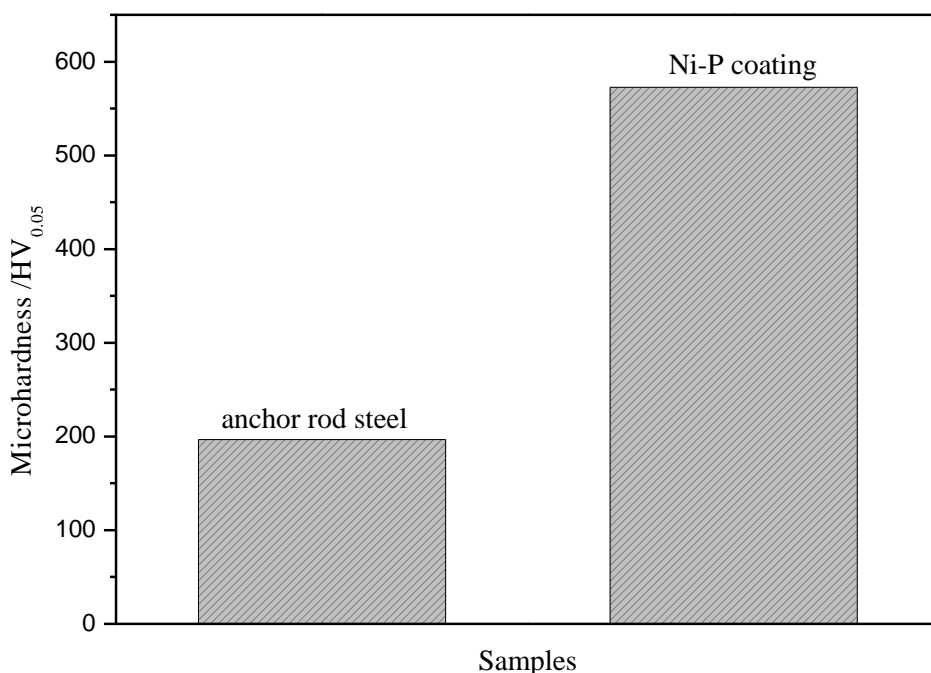


Figure 6. Surface microhardness of bare and Ni-P coated RB400 steel samples

3.3. Wear resistance of Ni-P coating

As the bolt wear under supporting engineering is fretting wear process, reciprocating and short distance wear test was chosen. Two pressure loads of 5N and 20N was set up to study the tribological properties respectively. The friction coefficient of the RB400 steel substrate and Ni-P coating under different loads are given in Figure 7. It is clear that the Ni-P coating has a lower friction coefficient than that of substrate steel. In the load condition of 5 N, the coefficient declined from 0.711 to 0.467, while the average value decreases from 0.396 to 0.283 in 20 N. The lower coefficient is attributed to

the amorphous structure showing a dense state of minuteness, which indicates a good antifriction effect of the deposited Ni-P coating. The mass losses of the bare sample and Ni-P coated sample after dry-sliding wearing (Figure 8) corroborate the experimental results of friction coefficient. The antifriction effect of Ni-P coating reveals the less mass lose, the result is more pronounced under a larger load as 20 N. Furthermore, it seems that there is a direct relation between the hardness and mass loss, leading to the fact that an operating wear mechanism is abrasive wear.

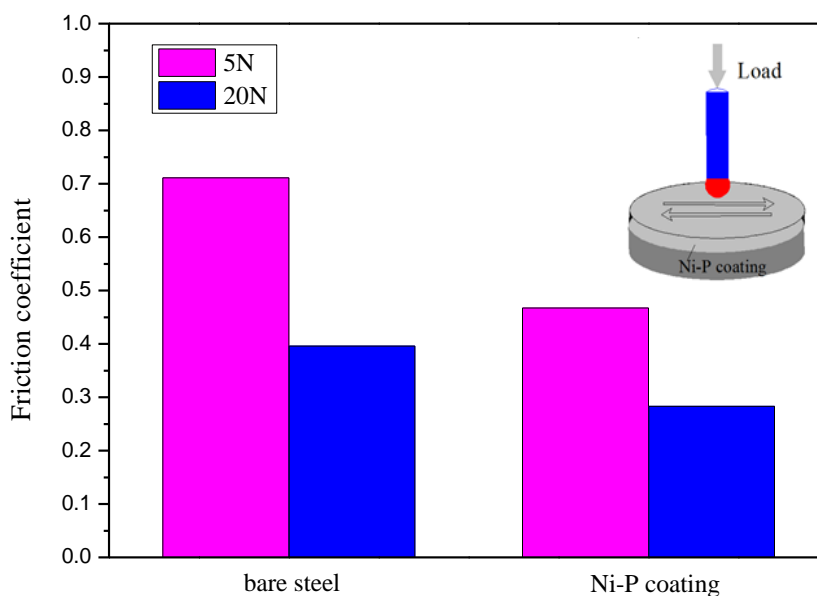


Figure 7. Friction coefficients of bare anchor rod substrate the Ni-P coating

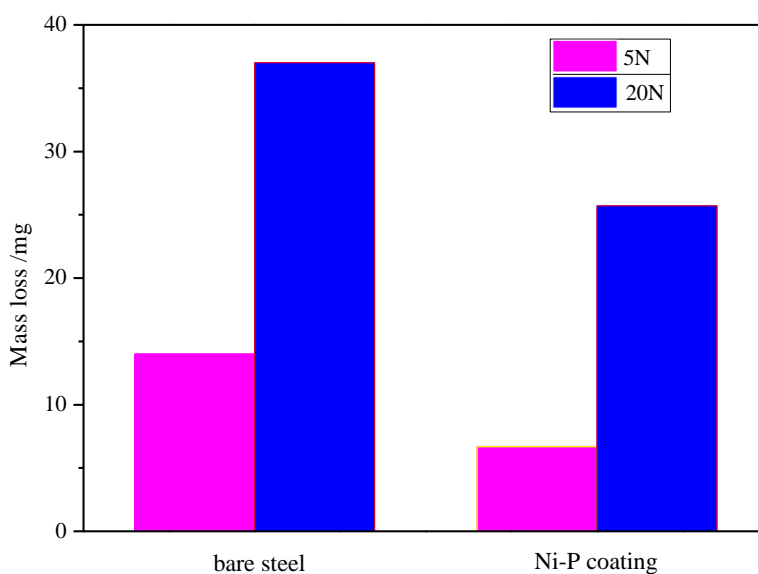


Figure 8. Mass loss of the bare anchor rod and Ni-P coating by dry-sliding wearing

Figures 9 and 10 show the wear scar morphologies of anchor rod substrate and Ni-P coating after the friction test under the load of 5 N and 20 N. When the load is 5N, after the wear action, the trace width of obtained Ni-P coating (Figure 9a) is obviously narrowed than that of the body steel (Figure 9c). The wear scar surface and width of the substrate (Figure 9a) appears uniform. Seen from Figure 9 b, the morphology is not flat at the magnification of 500. The worn surface of RB400 steel anchor rod is mainly composed of longitudinal grooves and partial irregular pits along the sliding direction. However, the wear degree of Ni-P coated sample is slight, few narrow ditches are seen towards the periphery of the wear track (Figure 9c). Figure 9d is the middle section of wear surface at high magnification, only shallow furrows and a small amount of debris can be seen in the picture. The surface appears relatively smoother than the substrate.

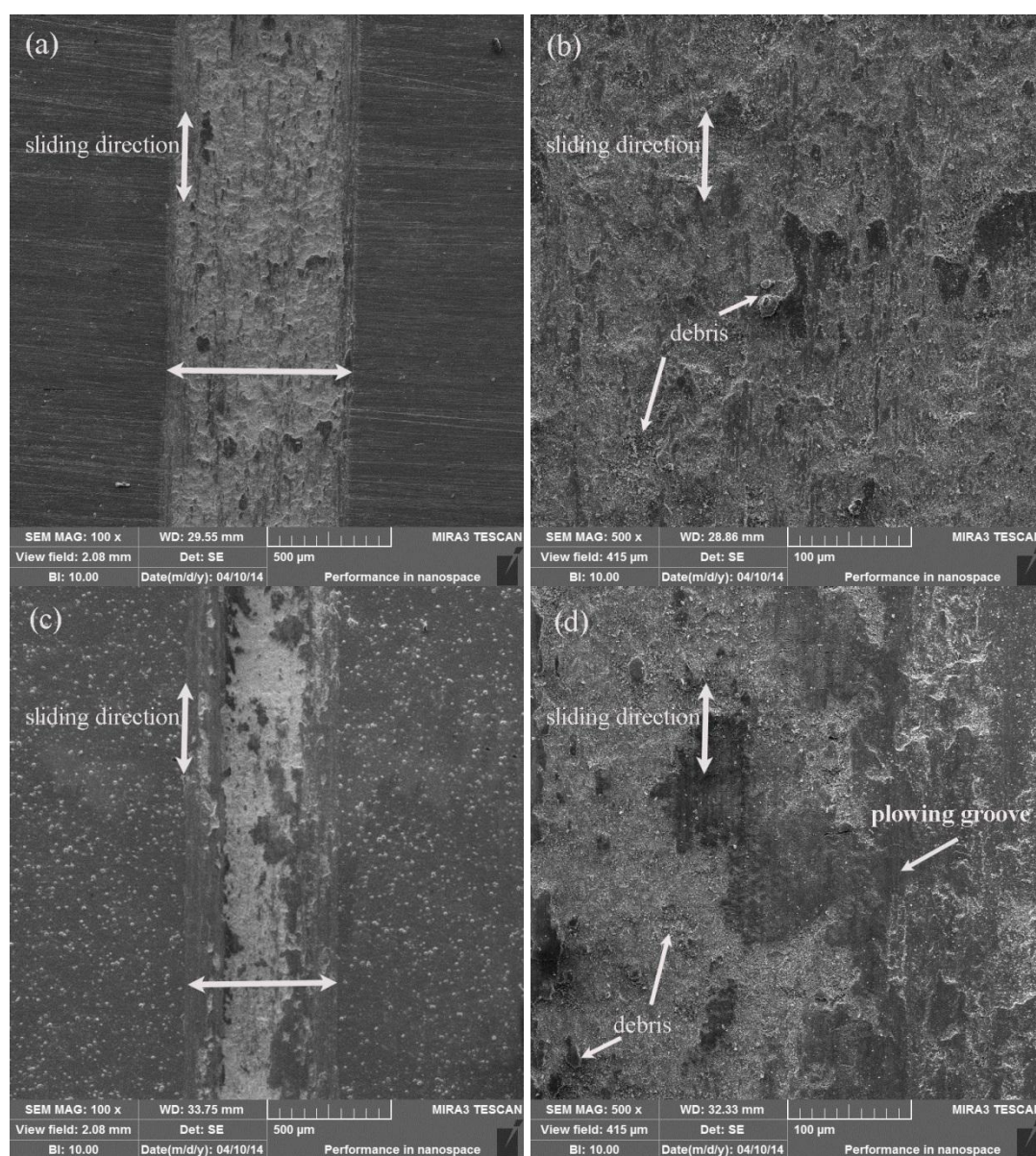


Figure 9. SEM images showing wore surface morphologies of raw material and the Ni-P coating under a load of 5 N (a)anchor rod 100× (b)anchor rod 500× (c)Ni-P coating 100× (d)Ni-P coating 500×

When the load is 20 N, Figure 10b shows the wear surface morphology of matrix. The falling debris even coalesces into patches, the ditches and microgrooves are the evidence of poor wear resistance. The trace width of Ni-P coated sample also becomes narrowed than the matrix (Figure 10c). There exist shallow furrows and light debris in Figure 10d. Overall, the damage extent of wear action to Ni-P coating is much lighter than the substrate. Due to the high hardness of Ni-P coating, the resistance to deformation of the Ni-P coating is stronger than the bare substrate. The ditched debris contributes to wear action [38]. When it is pressed by the friction counterparts, furrows are formed by the reciprocating wear of debris.

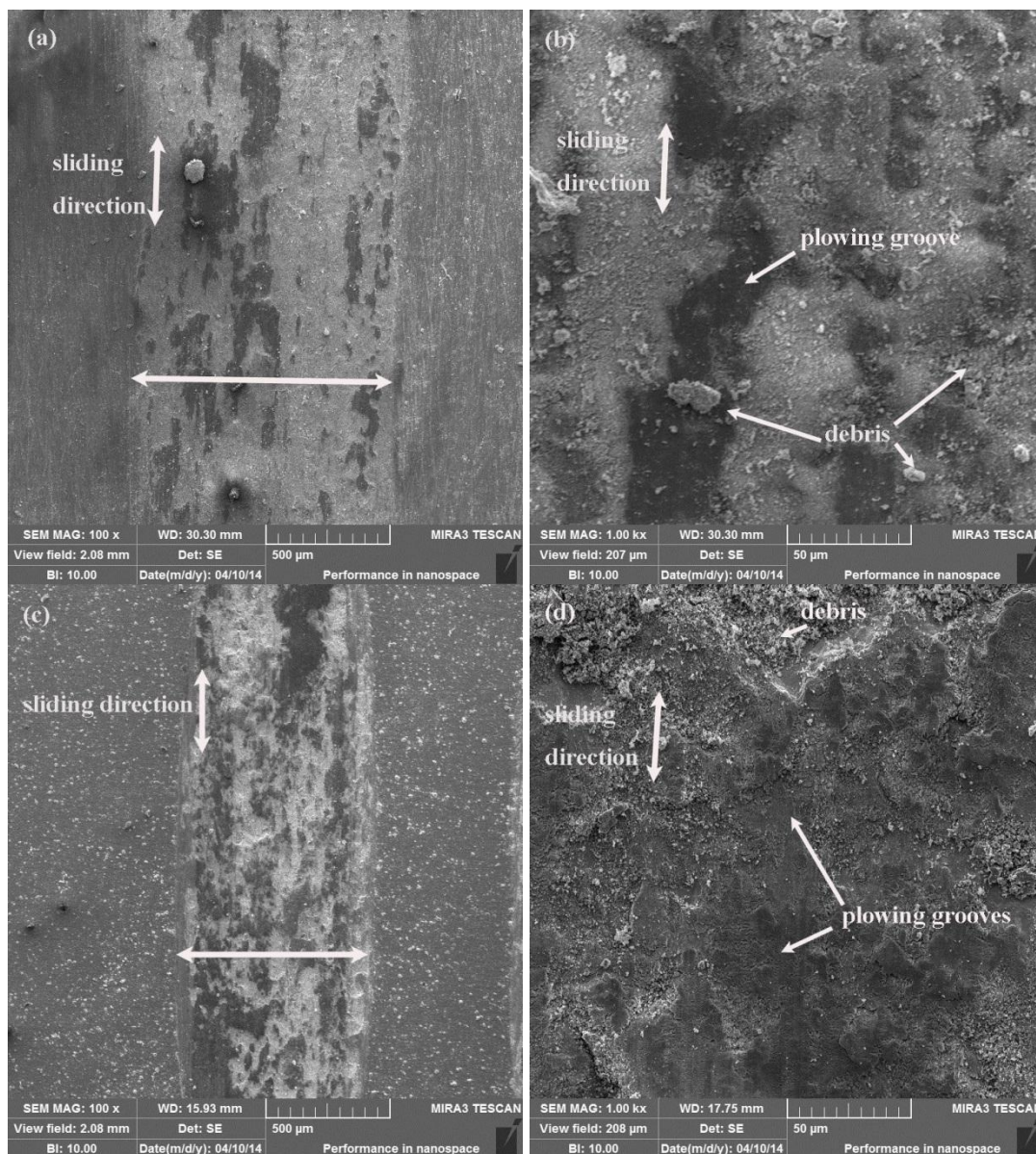


Figure 10. SEM images showing wore surface morphologies of raw material and the Ni-P coating under a load of 20 N (a)anchor rod 100× (b)anchor rod 1000× (c)Ni-P coating 100× (d)Ni-P coating 1000×

Furthermore, the behavior becomes more evidently under large load condition, so the worn surface morphology under the load of 20N seems severer than the one under the load of 5 N. The worn surface is mainly caused by the action of compressed falling debris. The wear mechanism of Ni-P coating is slight abrasive wear [39, 40]. The analysis coincides well with the previous mass loss results.

3.4. Corrosion resistance of Ni-P coating

The service environment of anchor bolt leads that its corrosion resistance has becoming a crucial factor affecting the application in some degree. The influence of chloride ions on corrosion resistance is more severe. In this experiment condition, the electrochemical performances of the two materials are evaluated by electrochemical experiments in 5 wt. % sodium chloride solution.

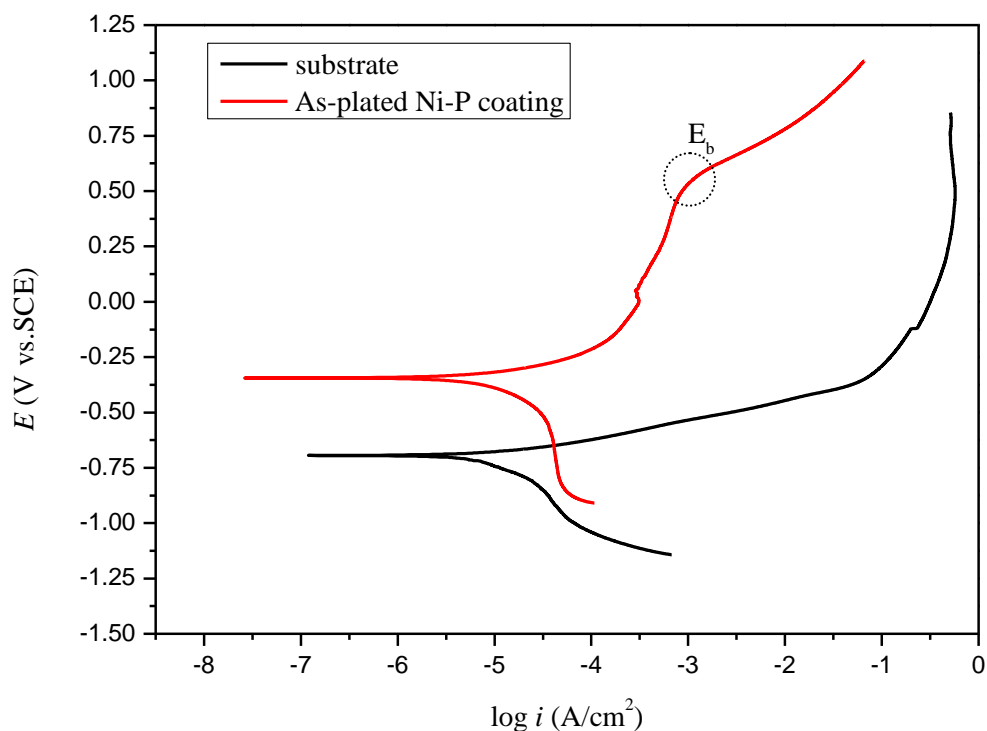


Figure 11. Electrochemical polarization curves of anchor rod substrate and as-plated Ni-P coating in 5 wt. % sodium chloride solution

The polarization curves of the RB400 steel and the deposited Ni-P coating are shown in Figure 11. It is clear that the corrosion potential (E_{corr}) of Ni-P coating is much higher than that of the bare steel. This can be expressed by another passivation parameter namely zero current potential (ZCP). It is recorded that the positive shift of ZCP is actually a consequence of the lower corrosion rate reducing the demand for cathodic current from the reduction of dissolved oxygen [41]. Moreover, in comparison to the substrate steel, the electroless plated Ni-P coating reveals a lower corrosion current density

(I_{corr}), which can be approached with the Tafel extrapolation method [42, 43]. Table 2 presents the detailed data. It can be found that the anodic and cathodic Tafel slopes of the Ni-P coating are steeper than that of the substrate, which means a smaller polarization resistance and obvious inhibition effect of Ni-P coating. It is noticed that the shift range in the anodic Tafel slopes of the tests is higher than the shift range in the cathodic Tafel slopes, which indicates that the decrease in the oxidation rate of the plated metal corresponds to the relative drop in the corrosion rate. The deviation of Tafel slopes from their actual values may be associated with scan rate and charging current disturbance [44]. Furthermore, as shown in Figure 11, the curve of Ni-P coating appears a passivation-like region in the potential range from 0 V to 0.5 V with lower corrosion current density than that of the substrate. With the increase of potential, the current increases slowly. The phenomenon shows that a passive film may be generated in the process. The passive film can provide some protection to the substrate and slow down the corrosion rate of materials. After the breakdown potential (E_b) marked in small circle, the rapid increase of current density indicates that the passive film is broken at that moment. However, the curve of bare steel shows no passive area, the surface film formed by the accumulation of corrosion products is loose and shows poor protection ability. Furthermore, the corrosion medium becomes yellowish green after the polarization test, indicating that iron cations may enter the solution [44]. These results mean that the Ni-P coating is much harder to be corroded than the bare RB400 substrate steel, so the corrosion resistance of RB400 steel is greatly improved by Ni-P coating.

Electrochemical impedance spectroscopy (EIS) is an important method for characterizing the corrosion resistance of materials. The micro process and mechanism of the whole electrochemical system can be obtained from the test. The open circuit potential test is conducted before the experiment in general conditions. Thus the system can achieve and maintain stable equilibrium state which is the precondition of impedance test. Figure 12 shows the Nyquist plots obtained for substrate steel and plated Ni-P coating in 5 wt. % sodium chloride solution at their respective open circuit potentials. The curves consist of a single semi-circle in the high frequency regions signifying that the electrode process is controlled by charge transfer process. The radius of the circular arc reflects the resistance force of charge transfer in the electrode process. The larger radius indicates greater charge transfer resistance and much slower electrode process of action. The curve deviates from normal semicircular track, this phenomenon is dispersion effect. It may be related with the inhomogeneity of the electrode surface, reflecting that the electric double layer capacitor deviates from the ideal. The occurrence of a single circle in the plots also indicates that the corrosion process involves a single time constant [45]. It can be seen that the curves exist shrinkage in the low frequency region, which imply the adsorption and drilling processes of chloride ion on the surface of the microporous film, leading to serious dispersion effect.

An equivalent electrical circuit model given in Figure 13 has been utilized to simulate the metal/ solution interface and to analyze the Nyquist plot. The charge transfer resistance R_{ct} and double layer capacitance C_{dl} obtained for the substrate and Ni-P coating are compiled in Table 2. The open circuit potential (OCP) is also included along with R_{ct} and C_{dl} values for effective comparison. The higher R_{ct} value of as-plated coating implies a good corrosion protective ability for the bare sample. The C_{dl} value may be related to the porosity of coating. The low C_{dl} value confirms that the plated Ni-P coating is relatively less porous in nature [46].

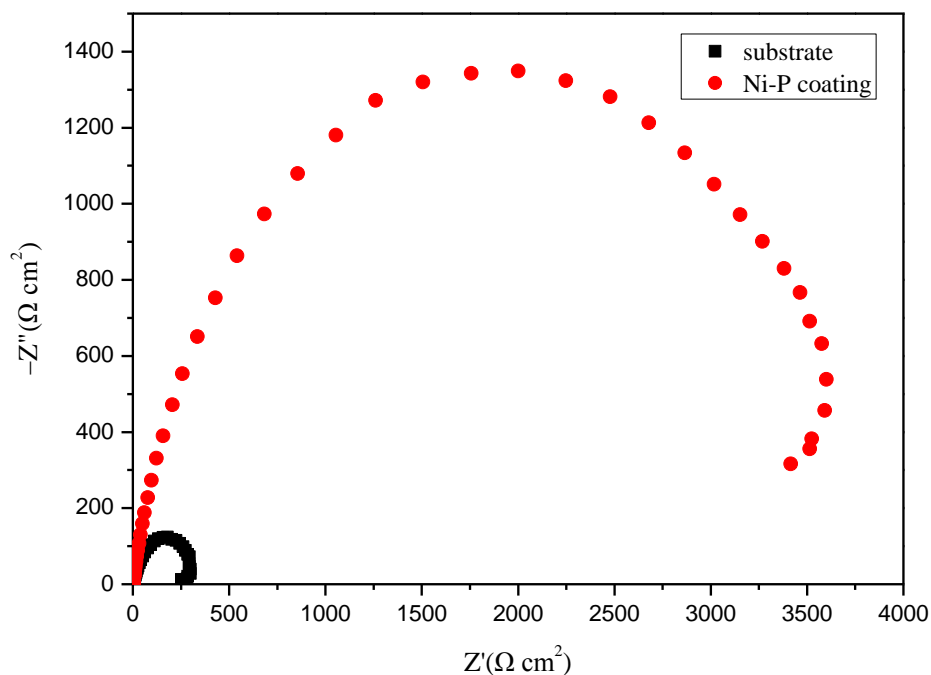


Figure 12. Nyquist plot for anchor rod substrate and as-plated Ni-P coating in 5 wt. % sodium chloride solution

Table 2. Electrochemical parameters of RB400 steel substrate and Ni-P coating from potentiodynamic polarization and EIS data in 5 wt. % sodium chloride solutions.

Samples	E_{corr} (V vs.SCE)	I_{corr} (A/cm ²)	β_c (mv/dec)	β_a (mv/dec)	OCP (V vs.SCE)	C_{dl} (μ F/cm ²)	R_{ct} ($\Omega \cdot$ cm ²)
substrate	-0.697	1.318×10^{-5}	394	86	-0.554	333.2	271.1
Ni-P coating	-0.343	4.456×10^{-6}	403	245	-0.421	33.05	3279

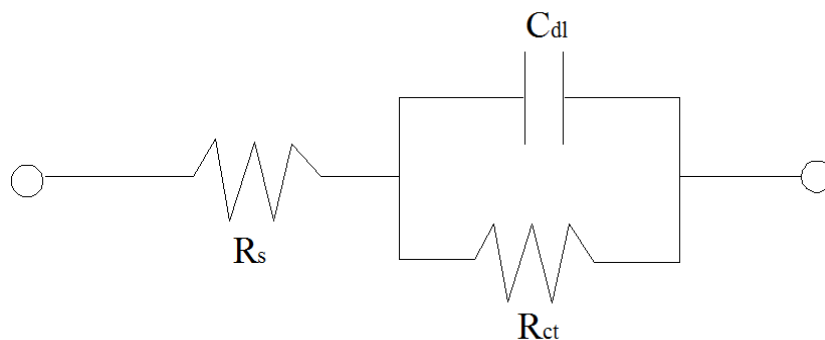


Figure 13. Equivalent electrical circuit model used to analyze the EIS data of plated Ni-P coating

Combining above polarization and impedance results, it can be concluded that the electroless Ni-P deposited anchor rods exhibit excellent corrosion resistance. As a barrier film, the electroless Ni-P protects the substrate from the corrosive environments by sealing its surface. The high resistance is a result of the amorphous nature and passivity of the Ni-P coating. Because the amorphous alloys are free of grain boundaries as well as glassy nature. They provide better corrosion protection than that of equivalent polycrystalline materials [47]. The formation mechanism of passivation film is reported as follows. Preferential dissolution of nickel occurs at open circuit potential, leading to the enriched phosphorous surface, which would react with water to form a layer of absorbed hypophosphite anions (H_2PO_2^-). This layer in turn will block the water supply to the metal surface, thereby preventing the hydration of nickel, which is considered to be the first step to form either soluble Ni^{2+} species or a nickel passive film [48, 490].

5. CONCLUSION

(1) A uniform and compact Ni-P coating has been deposited on RB400 steel anchor rod by electroless plating. The electroless plated Ni-P coating contains amorphous and microcrystalline nickel.

(2) The surface hardness of anchor rod has tripled through electroless Ni-P plating technique.

(3) The Ni-P coating indicates good antifriction effect and the Ni-P plated reinforced bar RB400 steel exhibits excellent wear resistance proved by the friction coefficient, wear loss and worn-out appearance. The wear mechanism of Ni-P coating is slight abrasive wear.

(4) The Ni-P coating indicates higher corrosion potential, lower current density and higher charge transfer resistance than the substrate. The anticorrosion performance of RB400 steel is improved effectively by electroless plating Ni-P coating on its surface, which is attributed to mechanical isolation and chemical stability of the Ni-P coating.

(5) The study confirmed that electroless plating can improve the performance of anchor rod. In order to achieve large-scale application and ensure the effect of electroless plating, it is strict requirement for the uniformity and stability of plating bath. Furthermore, analyzing and improving the bonding force between the coating and substrate is an important research field. Multiple and composite plating technology is a frontier field of electroless plating development, in future work, we will try to conduct the experiment through adding oxide nanoparticles or rare earth elements to further improve the coating performance on anchor bolt.

ACKNOWLEDGEMENTS

This work was supported by the National Natural Science Foundation of China (51208333), the China Postdoctoral Science Foundation (No.2012M520604), the Natural Science Foundation for Young Scientists of Shanxi Province (No.2013021013-2, No. 2014011036-1), the Youth Foundation of Taiyuan University of Technology (No.2012L050, No.2013T011) and the Qualified Personnel Foundation of Taiyuan University of Technology (QPFT) (No.tyut-rc201157a).

References

1. Y. Huang, Z.K. Guo and X.F. Xiang, *Geotech. Eng. Tech.* 18 (2004) 263.
2. http://www.e9898.com/tp/image_cp/201011/20101114114937187.jpg
3. <http://ok.pai-hang-bang.cn/wangdian-中空锚杆.html>
4. http://lq.zhulong.com/info_wiki/read654833.html
5. <http://www.youboy.com/pics73302241.html>
6. J. Zhao, W.Z. Ji, W.J. Zhang and X.M. Zeng, *Chin. J. Undergr. Space Eng.* 1 (2005) 1157.
7. J.H. Wang, X.M. Zeng and Q. Zhao, *Constr. Technol.* 35 (2006) 30.
8. L. Xiao, S.M. Li, X.M. Zeng and D.L. Lin, *Chin. J. Rock Mech. and Eng.* 27 (2008) 3791.
9. L. Maldonado, M.A. Pech-Canul and S. Alhassan, *Anti-Corros. Methods Mater.* 53 (2006) 357.
10. T. Bellezze, M. Malavolta, A. Quaranta, N. Ruffini and G. Roventi, *Cem. Concr. Compos.* 28 (2006) 246.
11. M. Manna, G. Naidu, N. Rani and N. Bandyopadhyay, *Surf. Coat. Technol.* 202 (2008) 1510.
12. J.S. Lawler, P.D. Krauss, J. Kurth and D. McDonald, *Transp. Res. Rec.: J. Transp. Res. Board*, 2220 (2011) 57.
13. R. Rajendran, W. Sha and R. Elansezhian, *Surf. Coat. Technol.* 205 (2010) 766.
14. Z.C. Shao, Z.Q. Cai, R. Hu and S.Q. Wei, *Surf. Coat. Technol.* 249 (2014) 42.
15. G.C. Liu, Z.X. Huang, L.D. Wang, W. Sun, S.L. Wang and X.L. Deng, *Surf. Coat. Technol.* 222 (2013) 25.
16. V.K. Bulasara, H. Thakuria, R. Uppaluri and M.K. Purkait, *Desalination* 268 (2011) 195.
17. S.M. Bak, K.H. Kim, C.W. Lee and K.B. Kim, *J. Mater. Chem.* 21 (2011) 1984.
18. W. Wang, S. Ji and I. Lee, *Appl. Surf. Sci.* 283 (2013) 309.
19. J. Sudagar, J. S. Lian and W. Sha, *J. Alloys Compd.* 571 (2013) 183.
20. J.N. Balaraju, T.S. Narayanan and S.K. Seshadri, *J. Appl. Electrochem.* 33 (2003) 807.
21. C. Gu, J. Lian, G. Li, L. Niu and Z. Jiang, *J. Alloy. Compd.* 391 (2005) 104.
22. Z. H. Xie, G. Yu, B. N. Hu, X. Y. Zhang, L. B. Li, W. G. Wang and D. C. Zhang, *Int. J. Electrochem. Sci.* 8 (2013) 6664.
23. M. Islam, M.R. Azhar, N. Fredj and T.D. Burleigh, *Surf. Coat. Technol.* 236 (2013) 262.
24. M. Yan, H.G. Ying and T.Y. Ma, *Surf. Coat. Technol.* 202 (2008) 5909.
25. Y.F. Shen, W.Y. Xue, Z.Y. Liu and L. Zuo, *Surf. Coat. Technol.* 205 (2010) 632.
26. Y.H. Cheng, Y. Zou, L. Cheng and W. Liu, *Surf. Coat. Technol.* 203 (2009) 1559.
27. C.K. Lee, Structure, *Mater. Chem. Phys.* 114 (2009) 125.
28. C.K. Lee, *Surf. Coat. Technol.* 202 (2008) 4868.
29. D.D.N. Singh and Rita Ghosh, *Surf. Coat. Technol.* 201 (2006) 90.
30. R. Ansari and A.H. Alikhani, *J. Coat. Technol. Res.* 6 (2009) 221.
31. M.M.H. Al-Tholaia, A.K. Azad, S. Ahmad and M.H. Baluch, *Constr. Build. Mater.* 56 (2014) 74.
32. M. Manna, N. Bandyopadhyay and D. Bhattacharjee, *Surf. Coat. Technol.* 202 (2008) 3227.
33. M. Gastaldi and L. Bertolini, *Cem. Concr. Res.* 56 (2014) 52.
34. B. Szczygieł, A. Turkiewicz and J. Serafińczuk, *Surf. Coat. Technol.* 202 (2008) 1904.
35. H. C. Jiang and C. Z. Yang, X-ray diffraction and scattering analysis of materials, Higher Education Press, Beijing (2010).
36. H. Ashassi-Sorkhabi and S.H. Rafizadeh, *Surf. Coat. Technol.* 176 (2004) 318.
37. M. Yan, H.G. Ying and T.Y. Ma, *Surf. Coat. Technol.* 202 (2008) 5909.
38. M. Franco, W. Sha, S. Malinov and H. Liu, *Wear*, 317 (2014) 254.
39. S. Zhang, K. Han and L. Cheng, *Surf. Coat. Technol.* 202 (2008) 2807.
40. X.H. Chen, C.S. Chen, H.N. Xiao, H.B. Liu, L.P. Zhou, S.L. Li and G. Zhang, *Tribol. Int.* 39 (2006) 22.
41. J. A. Liu, X. Y. Zhu, J. Sudagar, F. Gao and P. B. Feng, *Int. J. Electrochem. Sci.* 7 (2012) 5951.
42. P. Xu, C.X. Lin, C.Y. Zhou and X.P. Yi, *Surf. Coat. Technol.* 238 (2014) 9.

43. V. A. Alves, R.Q. Reis, I.C.B. Santos, D.G. Souza, T. de F. Goncalves, M.A. Pereira-da-Silva, A. Rossi and L.A. da Silva, *Corros. Sci.* 51 (2009) 2473.
44. W. Ye, Y. Li and F. H. Wang, *Electrochim. Acta* 54 (2009) 1339.
45. J. Balaraju, T.S. Narayanan and S. Seshadri, *J. Solid State Electrochem* 5 (2001) 334.
46. T. Rabizadeh, S.R. Allahkaram and A. Zarebidaki, *Mater. Des.* 31 (2010) 3174.
47. R.M. Abdel-Hameed and A.M. Fekry, *Electrochim. Acta* 55 (2010) 5922.
48. B. Elsener, M. Crobu, M.A. Scorciapino and A. Rossi, *J. Appl. Electrochem* 38 (2008) 1053.
49. B. Bozzoni, C. Lenardi, M. Serra and M. Faniglulio, *Br. Corros. J.* 37 (2002) 173.

© 2015 The Authors. Published by ESG (www.electrochemsci.org). This article is an open access article distributed under the terms and conditions of the Creative Commons Attribution license (<http://creativecommons.org/licenses/by/4.0/>).